



1 **Climate change threatens archeologically significant ice**  
2 **patches: insights into their age, internal structure, mass**  
3 **balance and climate sensitivity**

4

5 **Rune Strand Ødegård<sup>1</sup>, Atle Nesje<sup>2</sup>, Ketil Isaksen<sup>3</sup>,**  
6 **Liss Marie Andreassen<sup>4</sup>, Trond Eiken<sup>5</sup>, Margit Schwikowski<sup>6</sup>**  
7 **and Chiara Uglietti<sup>6</sup>**

8 [1]{Norwegian University of Science and Technology, Gjøvik, Norway}

9 [2]{University of Bergen, Bergen, Norway}

10 [3]{Norwegian Meteorological Institute, Oslo, Norway}

11 [4]{Norwegian Water Resources and Energy Directorate, Oslo, Norway}

12 [5]{Department of Geosciences, University of Oslo, Oslo, Norway}

13 [6]{Paul Scherrer Institute, Villigen, Switzerland}

14 Correspondence to: R.S. Ødegård (rune.oedegaard@ntnu.no)

15

16 **Abstract**

17 Despite numerous spectacular archaeological discoveries worldwide related to melting ice  
18 patches and the emerging field of glacial archaeology, governing processes related to ice  
19 patch development during Holocene and their sensitivity to climate change are still largely  
20 unexplored. Here we present new results from an extensive 6-year (2009-2015) field  
21 experiment at Juvfonne ice patch in Jotunheimen in central southern Norway. Our results  
22 show that the ice patch existed continuously since the late Mesolithic period. Organic-rich  
23 layers and carbonaceous aerosols embedded in clear ice shows ages spanning from modern at  
24 the surface to ca. 6200 BCE at the bottom. This is the oldest dating of ice in mainland  
25 Norway. Moss mats appearing along the margin of Juvfonne in 2014 were covered by the  
26 expanding ice patch about 2000 years ago. During the study period the mass balance record  
27 shows a strong negative balance, and the net balance is highly asymmetric over short  
28 distances. Snow accumulation is poorly correlated with winter precipitation and single storm



1 events may contribute significantly to the total winter balance. Snow accumulation is approx.  
2 20 % higher in the frontal area compared to the upper central part of the ice patch. The  
3 thermal regime in Juvfonne is similar to what is found close to the equilibrium line of nearby  
4 glaciers. There is sufficient melt water to bring the permeable snowpack to an isothermal state  
5 within a few weeks in early summer. Below the seasonal snowpack ice temperatures are  
6 between -2 and -4°C, similar to the surrounding permafrost terrain. Juvfonne has clear ice  
7 stratification of isochronic origin. The cumulative deformation of ice over millennia explain  
8 the observed curved layering in the basal parts of the ice patch, which makes it difficult to  
9 relate the present thickness to previous thickness of the ice patch. Ice deformation and surface  
10 processes (i.e. wind and melt water) may have caused significant displacement of artefacts  
11 from their original position. Thus the dating and position of artefacts cannot be used directly  
12 to reconstruct previous ice patch extent. In the perspective of surface energy and mass  
13 balance; ice patches are in the transition zone between permafrost terrain and glaciers. Future  
14 research will need to carefully address this interaction to build reliable models.

15

## 16 **1 Introduction**

17 The emergence of glacial archaeology is described by Andrews and Mackay (2012) and  
18 Dixon et al. (2014). In archaeology, the term ‘glacial archaeology’ or ‘snow patch  
19 archaeology’ refers to several alpine contexts in different regions of the world (Callanan,  
20 2010). The release of Ötzi’s 5300 year old body from the ice marked the beginning of a  
21 number of remarkable archaeological discoveries world-wide connected to melting ice and  
22 thawing permafrost in the high mountains (Spindler, 1994). Discoveries are known from the  
23 Alps (Suter et al., 2005; Grosjean et al., 2007), mummies in Greenland (Hansen et al., 1985)  
24 and the Andes Mountains (Ceruti, 2004), and from archaeological finds at retreating ice  
25 patches in North America (Farnell et al., 2004; Dixon et al., 2005; Lee, 2012; Brunswig, 2014).  
26 When analysing the number of artefacts on a global scale during the Holocene, there is a  
27 negative correlation between periods of glacial advance and the number of artefacts. This is  
28 particularly the case in the Alps and North America (Reckin, 2013), but a similar pattern is  
29 also found in Norway (Nesje et al., 2012). The question is if this is caused by changes in  
30 climate dependent preservation conditions or decreased human use of these areas in periods of  
31 cold climate.



1 In Norway, there has been an increasing focus on ice patches since the extreme melting in  
2 southern Norway in the autumn of 2006. There are about 3000 known artefact finds globally  
3 from ice patches. Most of these have melted out during the last three decades. Approximately  
4 2000 of these archaeological finds are in central southern Norway, making it by far the most  
5 find-rich region in the world (Curry, 2014, pers.comm. Lars Pilø).

6 Among the most spectacular finds is a Bronze Age leather shoe that melted out in late autumn  
7 2006 and a well-preserved tunic dated between 230-390 (Common Era) CE (Finstad and  
8 Vedeler, 2008; Vedeler and Jørgensen, 2013). The shoe was dated to be around 3400 years old  
9 (1429-1257 Before Common Era (BCE)), and is by far the oldest shoe found in Norway.  
10 Dates are given in calibrated ages (BCE/CE) including 1 sigma errors ( $\sigma$ ).

11 The geoscience of old ice patches is still in its infancy and the geoscience literature about ice  
12 patches is sparse compared to glacial archaeology. Within the glaciological community it is  
13 commonly differed between glaciers and snowfields and active or inactive ice (UNESCO,  
14 1970). Snowfields may be seasonal or perennial. Seasonal snowfields melt during the  
15 summer. Perennial snowfields exist for two years or more. Smaller ice bodies without  
16 significant movement may be remnants of a past active glacier or a perennial snowfield and  
17 are commonly referred to as glacierets. In this paper, we use ice patch for perennial  
18 snowfields and glacierets. Ice patches are, in contrast to glaciers, mostly stagnant and  
19 therefore, do not convey mass from an accumulation towards an ablation area. In fact, ice  
20 patches often do not exhibit distinct glacier facies such as a firn area. In the wet-snow zone,  
21 the transformation of snow to ice is fast by metamorphism and refreezing of melt water.  
22 (Kawasaki et al., 1993). Ice patches and surrounding terrain are generally underlain by  
23 permafrost (Haeberli et al., 2004). There are few studies related to the thermal regime, mass  
24 balance and dynamics (Sato et al., 1984; Fukui, 2003; Fukui and Iida, 2011; Eveland et al.,  
25 2013). Fujita et al. (2010) concluded that they exist below the altitude of the regional  
26 equilibrium-line altitude (ELA) of glaciers. A study by Glazirin et al. (2004) showed that they  
27 can modify the nearby wind field. The mentioned studies have documented feedbacks  
28 between ice patch size and both summer ablation and winter snow accumulation. The spatial  
29 variability of the turbulent fluxes in an alpine terrain is of particular interest to ice patches. Ice  
30 patches are influenced by advective heat transfer in summer (Essery et al., 2006; Pohl et al.,  
31 2006; Mott et al., 2015). The sensible heat flux is reported to be to twice the net radiation input  
32 for melting snow (Morris, 1989).



1 Despite some progress in these studies, the state of knowledge is not at a level to design  
2 reliable models of how ice patches have developed during the Holocene and to evaluate their  
3 sensitivity to future climate changes. The main objective of this study is to help fill this  
4 knowledge gap. A multi-disciplinary approach was chosen, combining a set of new  
5 geophysical data, radiocarbon dating, mass balance measurements and visual observations  
6 from two 30-70 m tunnels that was excavated into the central parts of the ice patch in order to  
7 better understand (1) the age, (2) the mass balance, (3) the thermal regime, (4) ice layering  
8 and deformation on Holocene time scale and finally (5) the physical processes relevant to  
9 artefact displacement and preservation.

10

## 11 **2 Field site and physical setting**

12 The presented research is based on a 6-year field experiment at Juvfonne ice patch, located in  
13 Jotunheimen in central southern Norway (Fig. 1 and 2, 61.676°N, 8.354°E). In this area  
14 archaeologists have so far identified more than 65 sites with finds related to ice patches, but  
15 many sites with potential finds have not been checked in the field. The archaeological finds  
16 are related to reindeer hunting. The snowfields are an important refuge for the reindeers  
17 during hot summer days, giving them relief from pestering insects. Juvfonne and the  
18 surrounding terrain is a well-preserved Iron Age hunting ‘station’ documented by more than  
19 600 registered wooden artefacts and 50 hunting blinds. Radiocarbon dating of artefacts shows  
20 ages in two separate time intervals, 246-534 CE and 804-898 CE (Nesje et al., 2012). The  
21 geoscience studies at Juvfonne started in 2009 (Ødegård et al., 2011). Nesje et al. (2012) gave  
22 a comprehensive presentation and discussion of archaeological finds in central southern  
23 Norway related to Late Holocene climate history.

24 The width of the ice patch is approx. 500 m and upslope length 350 m. Juvfonne had an area  
25 of 0.15 km<sup>2</sup> and ranged in altitude from 1839 to 1993 m a.s.l. in 2010 (Andreassen, 2011).  
26 The mean surface slope is 17 degrees and the ice patch has a north-easterly aspect.

27 Due to snowdrift by prevailing westerly winds during the accumulation season, Juvfonne is  
28 below the regional temperature-precipitation equilibrium-line altitude (TP-ELA). Annual  
29 surface mass balance measurements have been conducted on three glaciers (since 1949 at  
30 Storbreen and 1962 at Hellstugubreen and Gråsubreen) in the Jotunheimen mountain region  
31 (Andreassen et al., 2005; Andreassen and Winswold, 2012). Except for a transient mass  
32 surplus from 1989-1995 due to increased winter precipitation in this period, the glaciers have



1 lost mass. Map surveys and inventory data show a reduction in area of the glaciers in  
2 Jotunheimen of about 10 % from the 1960s to 2003 (Andreassen et al., 2008).

3 Juvfonne is well within the mountain permafrost zone. Present permafrost thicknesses at  
4 elevations where we find perennial ice patches ( $\sim$  1700 m a.s.l.) can be estimated to be more  
5 than 100 m. Observations of ground thermal regimes (Harris et al., 2009;Farbrot et al., 2011),  
6 bottom temperature of snow cover (BTS) (Ødegård, 1993;Isaksen et al., 2002;Farbrot et al.,  
7 2011) and geophysical surveys to delineate the altitudinal limit of the permafrost (Hauck et  
8 al., 2004;Isaksen et al., 2011) along with spatial numerical equilibrium and transient  
9 permafrost models (Hipp et al., 2012;Gisnås et al., 2013;Westermann et al., 2013;Gisnås et  
10 al., 2015) indicate a lower limit of permafrost at 1450-1600 m a.s.l in the area.

11 Juvfonne is at a distance of 750 m and at the same altitude as the permafrost boreholes (the  
12 P30 and 31 Permafrost and Climate in Europe (PACE) boreholes) and climate monitoring site  
13 at Juvvasshøe (Sollid et al., 2000)(see Fig. 2). The site has a record of ground temperatures  
14 and meteorological observations since September 1999. Mean annual air temperature for the  
15 period 2000-2015 is  $-3.5$  °C. At 15 m depth, the permafrost temperature ranges from a  
16 minimum of  $-3.1$  °C in 1999 to a maximum of  $-2.5$ °C recorded in 2008. The active layer  
17 thickness has varied between 2.0 and 2.4 m and permafrost thickness is estimated to exceed  
18 300 m (Isaksen et al., 2011). In 2008 an altitudinal transect of permafrost boreholes and  
19 adjacent air temperature measurements were installed in the area (Farbrot et al 2013).

20 For the period 1961-1990 the mean annual precipitation is estimated to be between  $800\text{mm a}^{-1}$   
21 and  $1000\text{mm a}^{-1}$  at 1900 m a.s.l. (Norwegian Meteorological Institute, unpublished data).

22 Results of analysis from sediment cores in the nearby Juvvatnet was used to reconstruct the  
23 glacier activity of Kjelebrea and Vesljuvbrea (Nesje et al., 2012) following the methodology  
24 described by Bakke et al. (2010). The results indicate that the late Holocene variations of  
25 these glaciers are largely in agreement with size variations of other glaciers in the  
26 Jotunheimen area (Matthews and Dresser, 2008;Nesje, 2009). Lichenometry suggests that the  
27 margin of Juvfonne extended  $\sim$ 250 m from its present position during the LIA maximum  
28 extent in the mid-18th century (Nesje et al., 2012).

29



## 1 **3 Methods**

### 2 **3.1 Georadar**

3 The ice patch was surveyed by a RAMAC georadar 23 September 2009 and 1 March 2012,  
4 using a high frequency antenna of 500 MHz. The dielectric constant of ice was set to be 3.2,  
5 giving a phase velocity of  $168 \text{ m } \mu\text{s}^{-1}$ . Georadar data and positioning data from the Global  
6 Navigation Satellite System (GNSS) were manually digitized to obtain a point dataset of ice  
7 thickness and bed topography. The point datasets were interpolated to get an ice thickness  
8 map and a digital terrain model (DTM) of the ice patch bed. Obvious artefacts caused by the  
9 interpolation technique were manually removed. Totally 40 independent control points gave  
10 an estimated standard deviation of 1.1 m, and a maximum error of 2.6 m.

### 11 **3.2 Laser scanning**

12 The ice patch and surrounding terrain was scanned with an air-borne laser on 17 September  
13 2011. The area was scanned with 5 points  $\text{m}^{-2}$  with accuracy better than 0.1 m. Aerial photos  
14 were taken on the same day. These data were used to produce a high quality DTM and  
15 orthophotos of the ice patch surface and surrounding terrain. The DTM was resampled to a  
16 resolution of 1 m.

### 17 **3.3 Mass balance and front measurements**

18 Standard surface mass balance measurements of winter accumulation (snow depth at 20-60  
19 sites and density at 1 site) and ablation (at 1-4 stakes) following standard methods for the  
20 melting seasons of 2010-2015 (Andreassen, 2011). Distance to the terminus has been  
21 measured from two points outside the ice patch (Fig. 3a) in August or early September using a  
22 laser distance meter.

23 The extent of the Juvfonne ice patch has been surveyed by foot with differential GNSS  
24 mounted on a back pack (Fig 3a, Table 1). Surveys have been done annually in August or  
25 September from 2010 to 2015, but the survey from 2012 was only done along the lower part  
26 due to snow conditions. Areal extent was also determined by digitising outlines from  
27 orthophotos from 2011 and from topographical maps from the Norwegian mapping  
28 authorities in 1981 and 2004. Furthermore, outlines from Landsat inventories from 1997 and  
29 2003 were used (Andreassen et al., 2008; Winsvold et al., 2014). The accuracy of the



1 differential GNSS are within 1m, the accuracy of the N50 within 5 m and the accuracy of the  
2 Landsat mapping within 30 m. The standard deviation in height of the GNSS measurements is  
3 on the range 10-20 cm giving  $\pm 2$  standard deviations of 0.6 m.

#### 4 **3.4 Meteorological measurements**

5 Hourly meteorological data was obtained from the automatic weather station (AWS) at  
6 Juvvasshøe (1894 m a.s.l.). It is the highest official meteorological station in Norway and is  
7 freely exposed and highly representative for this study. The first station was set up in 1999  
8 (Isaksen et al., 2003) and a new official weather station was established at the same site in  
9 June 2009. One additional station recording hourly snow depth was set up in autumn 2011 in  
10 front of Juvfonne (95 m from the eastern margin of the snowfield). Hourly data on snow  
11 depth is scarce in the high mountains in Scandinavia. Observed air temperature and wind  
12 speed on Juvvasshøe were compared against the 1971-2000 climatological normal based on  
13 interpolated air temperature data from seNorge (Engeset et al., 2004) and daily observations  
14 of wind speed from Fokstugu (973 m a.s.l.), 70 km NE of Juvvasshøe, which was the best  
15 nearby correlated meteorological station having long-time series.

16 A thermistor cable was installed in a 10 m deep borehole in 2009 to record ice temperatures.  
17 Temperatures were recorded every 3 hours until late September 2011 with an accuracy of 0.05  
18 °C (1 standard deviation). The entire thermistor cable melted out in September 2014. ).  
19 Additional thermistor measurements were made in the snow and ice at the onset of thaw in  
20 spring 2010.

#### 21 **3.5 Radiocarbon dating**

22 In May 2010, a 30 m long ice tunnel was excavated in the Juvfonne ice patch. During spring  
23 2012 a new 70 metre long tunnel was excavated into the central parts of the ice patch. The  
24 tunnels gave an excellent opportunity to verify the radar data and to collect organic material  
25 for Accelerator Mass Spectrometry (AMS) radiocarbon dating. Dateable organic material is  
26 available, but there are no continuous layers of organic material. Radiocarbons dating prior to  
27 2012 are published in (Ødegård et al., 2011; Nesje et al., 2012; Zapf et al., 2013). Conventional  
28  $^{14}\text{C}$  ages were calibrated using OxCal v4.2.4 software (Bronk Ramsey and Lee, 2013) with  
29 the IntCal13 calibration curve (Reimer et al., 2013).

30



1 The organic debris has been collected from the walls and below the floor of the ice tunnels (5  
2 samples from the tunnel excavated in 2010 and 5 samples from the tunnel excavated in 2012)  
3 and organic debris melting out at the front of which two datings are reported in this paper.  
4 Nine additional datings were published by Nesje et al. (2012).

5 The recently developed method for radiocarbon dating of ice utilizes the organic carbon  
6 fraction of carbonaceous aerosols scavenged from the atmosphere during snowfall and  
7 embedded into the ice matrix (Jenk et al., 2009; Sigl et al., 2009). This method was tested with  
8 11 samples from Juvfonne in 2011 by comparing for the first time  $^{14}\text{C}$  ages determined from  
9 carbonaceous particles with  $^{14}\text{C}$  ages conventionally obtained from organic remains found in  
10 the ice (Zapf et al., 2013). The 2011 samples are JUV1 and JUV2 adjacent to the dated  
11 organic-rich layers in the 2010 tunnel and a surface sample JUV3 (Table 2). In summer 2015  
12 five samples of clear ice were collected adjacent to the plant fragment layer located just above  
13 the bed in the tunnel excavated in 2012 (JUV0, Table 2 and 3). All blocks of ice ( $\sim 20 \times 15 \times$   
14  $10$  cm) were extracted with a pre-cleaned chainsaw and were subsequently divided into  
15 smaller pieces. All ice blocks were transported frozen to Paul Scherrer Institute (PSI,  
16 Switzerland), decontaminated in a cold room by removing the outer layer (0.3 mm) with a pre  
17 cleaned stainless steel band saw and by rinsing the ice samples with ultra-pure water in a class  
18 100 clean room (Jenk et al., 2007).

19 Insoluble carbonaceous particles are filtered onto preheated quartz fibre filters (Pallflex  
20 Tissuquartz, 2500QAO-UP) and combusted with a thermo-optical organic carbon/elemental  
21 carbon (OC/EC) analyser (Model4L, Sunset Laboratory Inc., USA), using a well-established  
22 protocol (Swiss\_4S) for OC/EC separation (Zhang et al., 2012). Analyses of  $^{14}\text{C}$  were  
23 conducted using the 200 kV compact radiocarbon system 'MICADAS' at the University of  
24 Bern (LARA laboratory), equipped with a gas ion source coupled to the Sunset instrument,  
25 allowing measuring  $^{14}\text{C}$  directly in  $\text{CO}_2$  of 3-100  $\mu\text{g C}$  with an uncertainty level as low as 1%  
26 (Ruff et al., 2010).

27 Dates are given in calibrated ages (BCE/CE) including 1 sigma errors ( $\sigma$ ).

28



## 1 **4 Results**

### 2 **4.1 Ice thickness and ice layering**

3 The bed reflection was clearly seen in the radar plots (see example in Fig. 4). In addition the  
4 ice layering was detected on most of the plots, probably due to density differences in the ice  
5 layers (air bubbles) (Hamran et al., 2009). Georadar soundings from 2009 revealed a  
6 maximum ice thickness of 17-19 m (Ødegård et al., 2011). The near-surface reflection  
7 horizons are nearly parallel to the present surface. At depth, curved reflection horizons are  
8 observed. In the ice tunnels the curved layers can be directly observed forming a distinct  
9 angular discontinuity with the surface-parallel ice layers (Fig. 5). The surface parallel layers  
10 have melted away since 2009 in the central and southern parts of the ice patch (Fig 6). The  
11 DTM obtained from laser scanning combined with the bottom topography from the georadar  
12 gave a volume of 710,000 m<sup>3</sup> in late August 2011 (mean thickness 5.6 m). The surface of  
13 Juvfonne in September 2011 was used as the reference surface for the depth map (Fig. 3b).  
14 The maximum depth was 16 m close to the inner part of ice tunnel excavated in 2012. In this  
15 area the surface slope is about 18 degrees.

16

### 17 **4.2 Mass balance, front changes and areal extent**

18 Only one of the mass balance stakes (J2) existed continuously from autumn 2009 to spring  
19 2015 (Figs. 7 and 8). Stake J2 is in the central part of the ice patch (Fig. 3a).

20 Snow sounding measurements (N=232) range from 0.6-4.8 m over the period 2010-2015.  
21 Mean snow depth is 2.6 m (1.2 m w.e.). Some years show a pattern where most snow  
22 accumulates on the leeward side of the prevailing wind the previous winter, but this is not  
23 consistent. Inter annual variation accounts for 66%. The accumulation was further  
24 investigated by analysing the deviation from mean each year. This dataset contains a  
25 significant trend with increased accumulation towards the front (Fig. 3c and Table 4). The  
26 difference between the upper central area and the front is 0.2 m w.e (Fig 3c), which  
27 corresponds to approx. 20% increase in accumulation.

28 The total mass loss is measured to 10 m of ice at the site of the thermistor measurements (Fig.  
29 3a). The 10-metre thermistor cable installed on the 29<sup>th</sup> of October 2009 melted out in mid-  
30 September 2014. The total mass loss at stake J2 was 10.5 m w.e. during the same period.



1 Elevation changes from September 2011 to September 2014 are shown in Fig. 3d. These  
2 results are based on the laser scanning in 2011 and differential GNSS-tracking in 2014. The  
3 measurements show a highly significant asymmetric pattern with close to zero surface  
4 elevation changes in the western part and surface lowering of 3-5 m in the eastern and central  
5 part of the ice patch. This strong gradient is measured over distance of just 200 m at  
6 approximately the same altitude. The part with most negative change has more than average  
7 accumulation.

8 Front change measurements were initiated in 2009 at JF1 and in 2010 at JF2 (Fig. 9). The  
9 measurements revealed that Juvfonne retreated in all years except in 2012 and 2015 where the  
10 ice patch increased its size due to excessive snow that formed a thin ice and snow layer  
11 around the margin. The total retreat 2009-2014 is -52 m measured from JF1 and over 2010-  
12 2014 the mean change is 44 m (-51m from JF1 and -38 m from JF2).

13 The annual extent measurements (2010-2015) show area fluctuations of the margin, varying  
14 from 0.101 km<sup>2</sup> (9 September 2014) to a maximum of 0.186 km<sup>2</sup> on 11 September 2015  
15 (Table 1). The extent measurements show that the ice patch shrinks and grows along the  
16 whole margin.

### 17 **4.3 Climate parameters**

18 Air temperature and wind speed at Juvvasshøe for the period 2000-2015 are outlined in Fig.  
19 10 a-b over the ablation season (June-September). The mean June-September air temperature  
20 in this period is 3.2 °C (1.0 °C above the 1971-2000 mean). Air temperatures, near-ground  
21 surface temperatures and frequency of days with daily mean air temperature above 0 °C (the  
22 two latter are not shown in Fig. 10) are high in summers 2002, 2003, 2006, 2011 and 2014,  
23 and especially 2006. Observations from nearby weather stations with long climate series  
24 reported record-breaking temperatures in late summer and autumn 2006. In the investigation  
25 period 2009-2015 the coldest summer was 2012, which was the only summer below the 1971-  
26 2000 mean (Fig. 10).

27 In general there is a high frequency (35-58 days per season) of strong breeze during the period  
28 2009-2015 (Fig. 10b). Comparing wind data from the AWS at Fokstugu indicates two to three  
29 times more frequent strong wind than 1971-2000 mean during the investigation period.  
30 Observed incoming short- and longwave radiation from Juvvasshøe (not shown) show no



1 clear patterns related to single summers, but 2011 peaks out as the summer with greatest  
2 incoming longwave radiation.

3 For snow accumulation or abrasion on ice patches wind speed and wind direction is crucial.  
4 Results reveal (not shown here) that strong wind is frequent during winter. There are great  
5 variations from year to year and between early and late winter in respect to frequency of  
6 strong gale and wind direction.

7

#### 8 **4.4 Snow measurements and modelling**

9 The automatic snow depth observations in front of Juvfonne show great hourly to daily  
10 variability and there is distinct different pattern of snow accumulation between the four winter  
11 seasons (Fig. 11). The greatest increase in snow depth during early and mid-winter in all years  
12 is related to storm events. This is also the case for strong snow depth decrease events (mainly  
13 due to abrasion). Comparing the observed and modeled snow depths (which not take into  
14 account redistribution of snow by wind), it is clear that much of the accumulation is not  
15 correlated with precipitation (Fig. 11). The modelled snow depth for Juvfonne was obtained  
16 from a precipitation/degree-day model operating on  $1 \times 1$  km<sup>2</sup> developed for a web-based  
17 system (<http://senorge.no/>) for producing daily snow maps for Norway (Engeset et al.,  
18 2004; Saloranto, 2012). A similar poor correlation ( $r^2=0.24$ ) is also found for very small  
19 glaciers in the Alps (Huss and Fisher, 2016)

20 The observed melt in central parts (J2) was compared with a degree-day model using typical  
21 values calculated from nearby glaciers (Fig. 7) (Laumann and Reeh, 1993). This modelling  
22 shows a quite good fit except the 2010 season. In this season the summer balance was about  
23 twice the outcome of the degree-day model.

24

#### 25 **4.5 Temperature of ice and permafrost**

26 Temperature measurements in Juvfonne reveal 10-m depth ice temperature in the range of -2  
27 to -4 °C (Fig. 12). The ice and snow temperature results show that the Juvfonne ice patch is  
28 cold-based and underlain by permafrost (Fig. 13). The measurements at 5-10 m depth in the  
29 ice are similar to the measurements in the nearby permafrost borehole at Juvvasshøe (Fig. 12).



1 In spring, the melt water percolates and refreezes in the snowpack until the snow is isothermal  
2 at a temperature close to 0°C. The surface melt water does not percolate through the level of  
3 the winter cold wave. The heat flow into the ice is gradually decreasing during the melt  
4 season. Superimposed ice forms at the level of impermeable ice.

5

#### 6 **4.6 Radiocarbon dating**

7 The AMS radiocarbon dating obtained from organic-rich layers and from carbonaceous  
8 aerosols embedded in clear ice in the Juvfonne ice patch shows ages spanning from modern at  
9 the surface to ca. 6200 BCE at the bottom (clear ice below the basal organic-rich layer), thus  
10 showing that Juvfonne has existed continuously during the last ~7500 yrs. So far, the basal ice  
11 in Juvfonne is the oldest dated ice in mainland Norway (Table 2).

12 In the tunnel opened in 2010 the AMS radiocarbon dating of organic matter embedded in the  
13 ice shows modern age in the top layer at the entrance, and ages ranging from 1218-1125 BCE  
14 to 945-987 CE inside the tunnel. These results were previously published in Nesje et al.  
15 (2012) and recalibrated for this study (Fig. 14).

16 In the tunnel opened in 2012 the AMS radiocarbon dating of five organic layers embedded in  
17 the ice about 70 m from the margin of the ice patch, yielded dates in chronological order from  
18 the base upwards, ranging from 4711-4606 BCE at the base to 53 BCE – 21 CE in the ceiling  
19 of the ice tunnel, approximately 2.5 m above the tunnel floor. The organic debris that yielded  
20 the oldest age was collected from the innermost part of the ice tunnel, about 0.3 m above the  
21 bed. The layer where the sample was retrieved could be followed close to the bed in the inner  
22 parts of the tunnel. The carbon dates on carbonaceous aerosols were sampled at the same  
23 location to the side and below the plant fragment layer (Table 3). The oldest dating is 6418-  
24 5988 BCE. The position of the sample site is marked on Fig. 3a.

25 In the autumn 2014, two *in-situ Polytrichum* moss mats melted out along the margin of  
26 Juvfonne south of the ice tunnel excavated in 2010. AMS radiocarbon dates of the two moss  
27 mats indicate that the moss was killed by the expanding margin of the ice patch about 2000  
28 years ago (1 BCE -54 CE – Poz-66166 and 5-68 CE – Poz-66167). Thus the minimum extent  
29 of the south-eastern part of the ice patch observed in September 2014 is most likely the  
30 smallest in 2000 years.



1 With the exception of one identified outlier, the obtained results from dating of carbonaceous  
2 aerosol particles in the ice could reproduce the expected ages very well (Zapf et al., 2013).  
3 This gives confidence that the age of organic debris in the ice is similar to the surrounding ice.

4

## 5 **5 Discussion**

6 The discussion focuses on the value of this research in the context of the long-term objective  
7 to develop models of mass balance and thermal regime on Holocene time scale at ice patches  
8 and surrounding terrain.

9 The discussion is organised in four sections: (1) the mass balance, (2) thermal regime, (3) ice  
10 layering and deformation on Holocene time scale and (4) the environmental processes  
11 relevant to artefact displacement and preservation.

### 12 **5.1 The mass balance**

13 Perennial ice patches are, due to their existence, located at sites with close to long-term zero  
14 mass balance. The inter-annual variability in summer and winter balance could be  
15 considerable, but the long-term changes in mass must be close to zero as long as they do not  
16 disappear or develop into a glacier. The 6-year record of mass balance gives some insight into  
17 the spatial and temporal variability of the mass balance.

18 The snow accumulation during the 6-year period (2010-2015) shows increased accumulation  
19 towards the front of the ice patch. This is probably a response to increased melt. Along the  
20 outer rim of Juvfonne the surface altitude changes (negative net balance) vary between less  
21 than 1m to nearly 5m within a 200 m distance at same altitude over a period of 3 years (Fig.  
22 3d). Field data is consistent with the interpretation of increased melting due to sensible and  
23 latent heat fluxes. Micro-meteorological investigations by Mott et al. (2011) of processes  
24 driving snow ablation in an alpine catchment show that advection of sensible heat cause  
25 locally increased ablation rates at the upwind edges of the snow patches.

26 The 2010 anomaly in the summer balance is most likely related to increased melt during  
27 periods with strong south and south-easterly winds (unsheltered direction for Juvfonne)  
28 combined with relatively high air temperatures and high relative humidity causing enhanced  
29 turbulent fluxes. This 2010 anomaly is probably the reason for the asymmetric net balance of  
30 Juvfonne (Fig. 6). Exceptionally large melt episodes have recently been reported from the



1 southern and western part of Greenland ice sheet in July 2012, where nonradiative energy  
2 fluxes (sensible, latent, rain, and subsurface collectively) dominated the ablation area surface  
3 energy budget during multiday episodes (Fausto et al., 2016).

4 The snow recording from the station in front of Juvfonne (95 m from the front) clearly  
5 illustrates the complexity of snow accumulation in this environment In front of Juvfonne  
6 abrupt changes in snow depth within hours dominate the series, causing great day-to-day  
7 variability. These changes seem to be mainly driven by the rate of wind speed and wind  
8 direction. One single storm events with westerly winds could account for almost 50% of the  
9 winter accumulation in less than 24 hours (Figure 11, 2014-15). Spring snow accumulation  
10 with insignificant wind drift could also influence mass balance, like the 2012 season.

## 11 **5.2 Ground and ice thermal regime**

12 Juvfonne consists of cold ice surrounded by permafrost terrain (Fig. 12). Perennial ice patches  
13 can be used as indicators of local (mountain) permafrost conditions. The physical background  
14 is that their ice cannot warm above 0°C in summer, but cool down far below 0°C during the  
15 cold season. Holocene permafrost modelling (Lilleøren et al., 2012) suggest that permafrost  
16 survived the highest areas of the Scandinavian mountains during the Holocene thermal  
17 maximum (HTM), and thus permafrost ice could be of Pleistocene age. Radiocarbon dates  
18 from Juvfonne show that the deepest central part of the ice patch contains carbonaceous  
19 particles embedded in the ice 6418-5988 BCE (JUV0\_5 - Table 2). This is a strong indication  
20 that Juvfonne has existed continuously since mid-Holocene, and the dating of the ice could  
21 offer strongly needed validation of Holocene permafrost models. Juvfonne could contain  
22 older ice, and it is most likely that ice patches at higher altitude contains older ice.

23 The thermal regime of the ice in Juvfonne is similar to what is found close to the equilibrium  
24 line of nearby glaciers (Sørdal, 2013; Tachon, 2015). The temperature measurements show  
25 that there is sufficient melt water to bring the permeable snowpack to an isothermal condition  
26 within a few weeks in early summer (Fig. 13). Below the seasonal snowpack, the ice remains  
27 cold during the summer with temperatures on the range -2 - -4°C at 5-10 m depth (Fig. 12).

## 28 **5.3 Ice layering and deformation on Holocene time scale**

29 In the central parts of the ice patch, a first order estimate of maximum basal shear stress is on  
30 the range of 30-45 kPa (no averaging of surface slope). Adding 5 m to the depth will increase



1 the shear stress to 40-60 kPa for the central part. The latter is probably close to the range for  
2 the last decades. The cumulative deformation of ice (maximum ~30-60 kPa basal shear  
3 stresses) over millennia explains the observed curved layering in the basal layer of the ice  
4 patch (Fig. 4). Cumulative ice deformation on a time scale of several millennia makes it  
5 difficult to relate the present thickness and slope of these layer to previous thickness of the  
6 ice patch.

7 The observed ice layers almost certainly represent surface of isochronic deposition. Within  
8 both ice tunnels in Juvfonne there are several organic/debris layers of uncertain origin. From  
9 the appearance of these layers, it is probably wind or water transported material or reindeer  
10 droppings. In the case of Juvfonne, there is a reasonable correlation between the age of the ice  
11 and the age of the organic layers (Zapf et al., 2013). This is necessarily not the case at other  
12 ice patches.

13 The empirical relation between basal shear stress and altitude range of glaciers was  
14 investigated by Haeberli and Hoelzle (1995) based on data from the European Alps. A basal  
15 shear stress of 15-20 kPa is in good agreement with the values for ice bodies with elevation  
16 ranges of 150m as at Juvfonne.

17

#### 18 **5.4 Artefact displacement and preservation**

19 From a cultural management perspective, there is particular interest in developing methods to  
20 identify sites of interest (Rogers et al., 2014) and a better understanding of the environmental  
21 treats (Callanan, 2015). The environmental treats are mainly related to subaerial exposure of  
22 artefacts. Especially leather artefacts, textiles and steering feathers of arrows are exposed to  
23 movement and decomposition short time after melt out. Wooden objects are more resistant.

24 The artefacts at Juvfonne have been found in permafrost terrain surrounding the ice patch,  
25 most of them are found in the front of the ice patch within a few tens of meters of the ice  
26 patch. The wooden artefacts range from 250-900 CE. Even during the extreme minimum in  
27 September 2014 (Fig. 6) there are no observations of artefacts melting out within the ice.

28 The exposure time to physical processes and microbial activity is critical to artefact  
29 decomposition. At Juvfonne there is a gradual increase in the ground exposure time  
30 depending on snow accumulation and melt over millennia. The oldest ice found so far is



1 6418-5988 BCE (JUV0\_5 - Table 2). At the eastern edge AMS radiocarbon dates show that  
2 the moss mats were covered (killed) by the expanding snowfield about 2000 years ago (Table  
3 2, Poz-56952). Lichenometry indicates that the front of Juvfonne extended ~250 m from its  
4 present position during the LIA maximum in the mid-18<sup>th</sup> century (Nesje et al., 2012). A  
5 photo of Juvfonne from around 1900 shows the front close to the expected LIA extent. These  
6 results constrain the extent of the ice patch since the mid-Holocene, but temporal and spatial  
7 variability need to be considered to assess the actual exposure time of artefacts.

8 Several radiocarbon dates of the top layer in 2010 (Fig. 4) show modern age. This means that  
9 artefacts found at Juvfonne have been sub-aerially exposed after the LIA but prior to 2009.  
10 Thus the dating and position of artefacts cannot be used directly to reconstruct previous ice  
11 patch extent.

12 Juvfonne and surrounding terrain is an active environment in terms of geomorphological  
13 processes. In particular, during the extreme melting in autumn 2014 several small  
14 accumulations of organic material/debris occurred at the upper margin of the ice patch.  
15 Within a few days, melt water moved this material to the front of the ice patch. Downslope  
16 movement of artefacts by melt water is certainly possible at Juvfonne. Finds at other ice  
17 patches in Jotunheimen supports this interpretation, where different pieces of the same  
18 artefact have been found along the direction of steepest slope. Textiles and leather objects are  
19 more likely transported by wind, and preservation at its original position is less likely. There  
20 are no finds of textiles or leather objects at Juvfonne.

21

## 22 **6 Conclusion**

23

24 Based on a 6-year field experiment on Juvfonne ice patch in central southern Norway, the  
25 following main conclusion could be drawn:

- 26 • Ice stratigraphic characteristics and radiocarbon dating strongly suggest that the  
27 Juvfonne ice patch was small or absent during Holocene thermal maximum, but  
28 existed continuously since ca. 6200 BCE (the late Mesolithic period) without  
29 disappearing or developing into a glacier with basal sliding. The oldest radiocarbon  
30 dates show that the deepest central part of the ice patch contains carbonaceous



- 1 particles embedded in the ice 6418-5988 BCE, which is the oldest dating of ice in  
2 mainland Norway.
- 3 • Radiocarbon dates show that the moss mats appearing in 2014 were covered (killed)  
4 by the expanding snowfield about 2000 years ago. The minimum extent observed in  
5 September 2014 at the south-eastern part is most likely the smallest ice patch in ~2000  
6 years.
  - 7 • A 6-year record of mass balance measurements shows a strong negative balance. The  
8 total mass loss at one site was 10.5 m w.e. Elevation changes are highly asymmetric  
9 over short distances, from close to zero to surface lowering of several meters. There is  
10 a significant increase in snow accumulation towards the front of approx. 20%  
11 compared to the upper central area. Assuming that this is a close to equilibrium  
12 situation, increased accumulation reflects increased melt. Locally increased ablation  
13 rates are probably caused by significant spatial variability of the sensible and latent  
14 heat fluxes. The melt anomaly in 2010 is most likely related to periods of strong  
15 south-easterly winds and high relative moisture boosting the turbulent fluxes.
  - 16 • The winter balance is poorly correlated with winter precipitation. One single storm  
17 events may contribute significantly to the winter balance.
  - 18 • The thermal regime of the ice in Juvfonne is similar to what is found close to the  
19 equilibrium line of nearby glaciers. Temperature measurements show that there is  
20 sufficient melt water to bring the permeable snowpack to an isothermal state within a  
21 few weeks in early summer. Below the seasonal snowpack, at 5-10 m depth, the ice  
22 remains cold with temperatures between -2 and -4°C. The cold ice is surrounded by  
23 permafrost terrain having similar ground temperatures.
  - 24 • Geophysical investigations show a clear stratification. The observed ice layers almost  
25 certainly represent surface of isochronic deposition. At depth, curved reflection  
26 horizons are observed consistent with cumulative ice deformation over millennia.  
27 Even a thin ice patch like Juvfonne (<20 m thick) ice deformation is a critical factor in  
28 the interpretation of the ice layering and makes it difficult to relate the present  
29 thickness and slope of these layer to previous thickness of the ice patch.
  - 30 • Ice deformation and surface processes (i.e. wind and melt water) may have caused  
31 significant displacement of artefacts from their original position.



1       • Artefacts melted out in front of Juvfonne since 2009 have been sub-aerially exposed  
2           after the LIA but prior to 2009. Thus the dating and position of artefacts cannot be  
3           used directly to reconstruct previous ice patch extent.

4   The exploratory analyses of field data from Juvfonne show for the first time the geoscience  
5   research potential of ice patches in Scandinavia. The results give new insights into their age,  
6   internal structure, mass balance and climate sensitivity, and have taken the state of knowledge  
7   to level where models can be designed. The feedback mechanisms observed on Juvfonne  
8   suggest that ice patches are robust to climate change, at least on the time scale of decades.  
9   Perennial ice patches are, due to their existence, areas with close to long-term zero mass  
10   balance. However, they are probably more sensitive than glaciers to changes in the wind  
11   pattern. In the perspective of surface energy and mass balance; ice patches are in the transition  
12   zone between permafrost terrain and glaciers. Future research will need to carefully address  
13   this interaction to build reliable models of how ice patches have developed during the  
14   Holocene and their response to future climate change.

15

## 16   **Acknowledgements**

17   We thank the archaeologists Lars Pilø and Espen Finstad for valuable comments and  
18   discussions related to artefact displacements and Dag Inge Bakke at Mimisbrunnr Klimapark  
19   2469 for support in the field. Professor Emeritus Wilfried Haeberli and Professor Bernd  
20   Etzelmüller gave useful comments to an earlier version of the manuscript and are gratefully  
21   acknowledged.

22



## 1 **References**

2

3 Andreassen, L. M., Elvehøy, H., Kjølmoen, B., Engeset, R. V., and Haakensen, N.: Glacier  
4 mass-balance and length variations in Norway, *Ann Glaciol*, 42, 317-325, 2005.

5 Andreassen, L. M., Paul, F., Kääh, A., and Hausberg, J. E.: Landsatderived glacier inventory  
6 for Jotunheimen, Norway, and deduced glacier changes since the 1930s, *The Cryosphere*, 2,  
7 131-145, 2008.

8 Andreassen, L. M.: Glaciological investigations in Norway in 2010 - Juvfonne, NVE report 3,  
9 B. Kjølmoen (ed), 54-57, 2011.

10 Andreassen, L. M., and Winswold, S. H.: *Inventory of Norwegian Glaciers*, 236 pp., 2012.

11 Andrews, T. D., and Mackay, G.: *The Archaeology and Paleoecology of Alpine Ice Patches:  
12 A Global Perspective*, *ARCTIC*, 65, 4 pp., 2012.

13 Bakke, J., Dahl, S. O., Paasche, Ø., Riis Simonsen, J., Kvisvik, B., Bakke, K., and Nesje, A.:  
14 A complete record of Holocene glacier variability at Austre Okstindbreen, northern Norway:  
15 an integratd approach, *Quaternary Science Reviews*, 29, 1246-1262, 2010.

16 Bronk Ramsey, C., and Lee, S.: *Recent and Planned Developments of the Program OxCal*,  
17 *Radiocarbon*, 55, 2013.

18 Brunswig, R. H.: *Risks and Benefits of Global Warming and the Loss of Mountain Glaciers  
19 and Ice Patches to Archeological, Paleoclimate, and Paleoecology Resources*, *Ecological  
20 Questions*, 20, 99-108, 2014.

21 Callanan, M.: *Northern Snow Patch Archaeology, A Circumpolar Reappraisal: The Legacy of  
22 Gutorm Gjessing (1906-1979). Proceedings of an International Conference held in  
23 Trondheim, Norway, 10th-12th October 2008.*, Oxford, 2010,

24 Callanan, M.: *Managing the frozen heritage: Some challenges and responses*, *Quaternary  
25 International*, in press, 8 pp., 2015.

26 Ceruti, C.: *Human bodies as objects of dedication at Inca mountain shrines, north-western  
27 Argentina*, *World Archaeology*, 36, 103-122, 2004.

28 Curry, A.: *Racing the thaw*, *Science*, 346, 157-159, 2014.

29 Dixon, E. J., Callanan, M., Hafner, A., and Hare, G. P.: *The Emergence og Glacial  
30 Archaeology*, *Journal of Glacial Archaeology*, 1, 1-9, 2014.

31 Dixon, J., Manley, W. E., and Lee, C. M.: *The emerging archaeology of glaciers and ice  
32 patches*, *American Antiquity*, 70, 129-143, 2005.

33 Engeset, R. V., Tveito, O. E., Alfnes, E., Mengistu, Z., Udnæs, H.-C., Isaksen, K., and  
34 Førland, E. J.: *Snow Map System for Norway, XXIII Nordic Hydrological Conference 2004,  
35 Proceedings*, 8-12 August 2004, Tallinn, Estonia, 2004,

36 Essery, E., Ganger, R., and Pomeroy, J.: *Boundary-layer growth and advection of heat over  
37 snow and soil patches: modelling and parameterization*, *Hydrol. Processes*, 20, 953-967,  
38 10.1002/hyp.6122, 2006.



- 1 Eveland, J. W., Gooseff, M. N., Lampkin, D. J., Barrett, J. E., and D., T.-V. C.: Seasonal  
2 controls on snow distribution and aerial ablation at the snow patch and landscape scales  
3 McMurdo Dry Valleys, Antarctica, *The Cryosphere*, 7, 917–913, 2013.
- 4 Farbrot, H., Hipp, T., Etzelmuller, B., Isaken, K., Ødegård, R. S., Schuler, T. V., and  
5 Humlum, O.: Air and Ground Temperatures Variations Observed along Elevation and  
6 Continentality Gradients in Southern Norway, *Permafrost Periglacial Processes*,  
7 10.1002/ppp.733, 2011.
- 8 Farnell, R., Hare, G. P., Blake, E., Bowyer, V., Schweger, C., Greer, S., and Gotthardt, R.,  
9 2004. . *Arctic* 57(3), 247–259.: Multidisciplinary investigations of alpine ice patches in  
10 Southwest Yukon, Canada: paleo-environmental and paleobiological investigations, *ARCTIC*,  
11 57, 247-259, 2004.
- 12 Fausto, R. S., van As, D., Box, J. E., Colgan, W., Langen, P. L., and Mottram, R. H.: The  
13 implication of nonradiative energy fluxes dominating Greenland ice sheet exceptional  
14 ablation area surface melt in 2012, *Geophys. Res. Lett.*, 43, 10 pp.,  
15 doi:10.1002/2016GL067720, 2016.
- 16 Finstad, E., and Vedeler, M.: En bronsealdersko fra Jotunheimen, *Viking*, 71, 61-70, 2008.
- 17 Fujita, K., Hiyama, K., Iida, H., and Ageta, Y.: Self-regulated fluctuations in the ablation of a  
18 snow patch over four decades, *Water Resour. Res.*, 46, 9, doi:10.1029/2009WR008383, 2010.
- 19 Fukui, K.: Permafrost and surface movement of an active protalus rampart in the Kuranosuke  
20 Cirque, the Northern Japanese Alps, *Permafrost Conference*, Zurich, 2003.
- 21 Fukui, K., and Iida, H.: Flow of the ice body in the Gozenzawa perennial snow patch, the  
22 Tateyama Mountains, central Japan, *Japan Geoscience Union Meeting* 2011,
- 23 Gislén, K., Etzelmuller, B., Farbrot, H., Schuler, T. V., and Westermann, S.: CryoGRID 1.0:  
24 Permafrost Distribution in Norway estimated by a Spatial Numerical Model, *Permafrost*  
25 *Periglacial Processes*, 24, 2-19, Doi 10.1002/ppp.1765, 2013.
- 26 Gislén, K., Westermann, S., Schuler, T. V., Melvold, K., and Etzelmuller, B.: Small-scale  
27 variation of snow in a regional permafrost model, *The Cryosphere Discuss.*, 9, 6661-6696,  
28 2015.
- 29 Glazirin, G. E., Kodama, Y., and Ohata, T.: Stability of drifting snow-type perennial snow  
30 patches, *Bull. Glaciol. Res.*, 21, 1-8, 2004.
- 31 Grosjean, M., Suter, P. J., Trachsel, M., and Wanner, H.: Ice-borne prehistoric finds in the  
32 Swiss Alps reflect Holocene glacier fluctuations, *J. Quat. Sci.*, 22, 203-207, 2007.
- 33 Haeblerli, W., and Hoelzle, M.: Application of inventory data for estimating characteristics of  
34 and regional climate-change effects on mountain glaciers: a pilot study with the European  
35 Alps, *J GLACIOL*, 21, 206-212, 1995.
- 36 Haeblerli, W., Frauenfelder, R., Käab, A., and Wagner, S.: Characteristics and potential  
37 climatic significance of “miniature ice caps” (crest- and cornice-type low-altitude ice  
38 archives), *J GLACIOL*, 50, 129-136, 2004.
- 39 Hamran, S.-E., Øyan, M. J., and Kohler, J.: UWB radar profiling reveals glacier facies, In  
40 proceedings of the 5th International Workshop on advanced GPR, Granada, Spain, 2009,
- 41 Hansen, J. P. H., Meldgaard, J., and Nordquist, J.: Qilakitsoq. De Grønlandske mumier fra  
42 1400-tallet, Nuuk and Copenhagen: Grønlands Landsmuseum/Christian Ejlers' forlag, 216  
43 pp., 1985.



- 1 Harris, C., Arenson, L. U., Christiansen, H. H., Etmüller, B., Frauenfelder, R., Gruber, S.,  
2 Haeberli, W., Hauck, C., Holzle, M., Humlum, O., Isaksen, K., Kaab, A., Kern-Lutschg, M.  
3 A., Lehning, M., Matsuoka, N., Murton, J. B., Nozli, J., Phillips, M., Ross, N., Seppala, M.,  
4 Springman, S. M., and Muhl, D. V.: Permafrost and climate in Europe: Monitoring and  
5 modelling thermal, geomorphological and geotechnical responses, *Earth Sci. Rev.*, 92, 117-  
6 171, 10.1016/j.earscirev.2008.12.002, 2009.
- 7 Hauck, C., Isaksen, K., Vonder Mühll, D., and Sollid, J. L.: Geophysical surveys designed to  
8 delineate the altitudinal limit of mountain permafrost: an example from Jotunheimen,  
9 Norway, *Permafrost Periglac.*, 15, 191-205, 2004.
- 10 Hipp, T., Etmüller, B., Farbrøt, H., Schuler, D. V., and Westermann, S.: Modelling  
11 borehole temperatures in Southern Norway – insights into permafrost dynamics during the  
12 20th and 21st century, *Cryosphere*, 6, 553-571, 2012.
- 13 Huss, M., and Fisher, M.: Sensitivity of Very Small Glaciers in the Swiss Alps to Future  
14 Climate Change, *Front. Earth Sci.*, 4, 17 pp., 10.3389/feart.2016.00034, 2016.
- 15 Isaksen, K., Hauck, C., Gudevang, E., Ødegård, R. S., and Sollid, J. L.: Mountain permafrost  
16 distribution on Dovrefjell and Jotunheimen, southern Norway, based on BTS and DC  
17 resistivity tomography data, *Norsk Geografisk Tidsskrift*, 56, 122-136, 2002.
- 18 Isaksen, K., Heggem, E. S. F., Bakkehøi, S., Ødegård, R. S., Eiken, T., Etmüller, B., and  
19 Sollid, J. L.: Mountain permafrost and energy balance on Juvvasshøe, southern Norway, In  
20 *Proceedings Volume 1, Eight International Conference on Permafrost*, Zurich, Switzerland,  
21 21–25 July, 467-472, 2003.
- 22 Isaksen, K., Ødegård, R. S., Etmüller, B., Hilbich, C., Hauck, C., Farbrøt, H., Eiken, T.,  
23 Hygen, H. O., and Hipp, T.: Degrading mountain permafrost in southern Norway - spatial and  
24 temporal variability of mean ground temperatures 1999-2009, *Permafrost Periglacial*  
25 *Processes*, 22, 361-377, 2011.
- 26 Jenk, T. M., Szidat, S., Schwikowski, M., Gaggeler, H. W., Wacher, L., Synal, H.-A., and  
27 Sauer, M.: Microgram level radiocarbon ( $^{14}\text{C}$ ) determination on carbonaceous particles in  
28 ice, *Nuclear Instruments and Methods in Physics Research B* 259, 518-525, 2007.
- 29 Jenk, T. M., Szidat, S., Bolius, D., Sigl, M., Gaggeler, H. W., Wacker, L., Ruff, M., Barbante,  
30 C., Boutron, C. F., and Schwikowski, M.: A novel radiocarbon dating technique applied to an  
31 ice core from the Alps indicating late Pleistocene ages, *J. Geophys. Res.*, 114,  
32 10.1029/2009JD011860, 2009.
- 33 Kawasaki, K., Yamada, T., and Wakahama, G.: Investigation of internal structure and  
34 transformational processes from firn and ice in a perennial snow patch, *Ann Glaciol.*, 18, 117-  
35 122, 1993.
- 36 Laumann, T., and Reeh, N.: Sensitivity to climate change of the mass balance of glaciers in  
37 southern Norway, *J GLACIOL.*, 39, 656-665, 1993.
- 38 Lee, C. M.: Withering snow and ice in the mid-latitudes: A new archaeological and  
39 paleobiological record for the Rocky Mountain region, *ARCTIC*, 165-177, 2012.
- 40 Lilleøren, K., Etmüller, B., Schuler, D. V., Gislås, K., and Humlum, O.: The relative age  
41 of mountain permafrost - estimation of Holocene permafrost limits in Norway *Global Planet.*  
42 *Change*, 92-93, 209-223, 2012.



- 1 Matthews, J. A., and Dresser, P. Q.: Holocene glacier variation chronology of the  
2 Smørstabbtinden massif, Jotunheimen, southern Norway, and the recognition of century- to  
3 millennial-scale European Neoglacial events, *The Holocene*, 18, 181-201, 2008.
- 4 Morris, E. M.: Turbulent Transfer over Snow and Ice, *Journal of Hydrology*, 105, 205-223,  
5 1989.
- 6 Mott, R., Egli, L., Grunewald, T., Dawes, N., Manes, C., Bavay, M., and Lehning, M.:  
7 Micrometeorological processes driving snow ablation in an Alpine catchment, *The*  
8 *Cryosphere*, 5, 1083-1098, 2011.
- 9 Mott, R., Daniels, M., and Lehning, M.: Atmospheric Flow Development and Associated  
10 Changes in Turbulent Sensible Heat Flux over Patchy Mountain Snow Cover, *J*  
11 *Hydrometeorol*, 16, 1315-1340, 2015.
- 12 Nesje, A.: Latest Pleistocene and Holocene alpine glacier fluctuations in Scandinavia. ,  
13 *Quaternary Science Reviews*, 28, 2119-2136, 2009.
- 14 Nesje, A., Pilø, L. H., Finstand, E., Solli, B., Wangen, V., Ødegård, R. S., Isaken, K., Støren,  
15 E., Bakke, D. I., and Andreasse, L. M.: The climatic significance of artefacts related to  
16 prehistoric reindeer hunting exposed at melting ice patches in southern Norway, *The*  
17 *Holocene*, 22, 485-496, 2012.
- 18 Pohl, S., Marsh, P., and Liston, G. E.: Spatial-Temporal Variability in Turbulent Fluxes  
19 during Spring Snowmelt, *ARCT ANTARCT ALP RES*, 38, 136-146, 2006.
- 20 Reckin, R.: Ice Patch Archaeology in Global Perspective: Archaeological Discoveries from  
21 Alpine Ice Patches Worldwide and Their Relationship with Paleoclimates, *Journal of World*  
22 *Prehistory*, 26, 63 pp., 10.1007/s10963-013-9068-3, 2013.
- 23 Reimer, P. J., Barad, E., Baykuss, A., Beck, J. W., Blackwell, P. G., Bronk Ramsey, C., Buck,  
24 C. E., Cheng, H., Edwards, R. L., Friedrich, M., Grootes, P. M., Guilderson, T. P.,  
25 Hafliadason, H., Hajdas, I., Hatté, C., Heaton, T. J., Hoffmann, D. L., Hogg, A. G., Hughen, K.  
26 A., Kaiser, K. F., Kromer, B., Manning, S. W., Niu, M., Reimer, R. W., Richards, D. A.,  
27 Scott, E. M., Southon, J. R., Staff, R. A., Turney, C. S. M., and van der Plicht, J.: IntCal13  
28 and Marine13 radiocarbon age calibration curves 0-50,000 years cal BP, *Radiocarbon*, 55,  
29 1869-1887, 2013.
- 30 Rogers, S. R., Fisher, M., and Huss, M.: Combining glaciological and archaeological methods  
31 for gauging glacial archaeological potential, *Journal of Archaeological Science*, 52, 410-420,  
32 2014.
- 33 Ruff, M., Fahrni, S., Gäggeler, H. W., Hajdas, I., Suter, M., Synal, H.-A., Szidat, S., and  
34 Wacker, L.: On-line radiocarbon measurements of small samples using elemental analyzer  
35 and MICADAS gas ion source, *Radiocarbon*, 52, 1645-1656, 2010.
- 36 Saloranto, T. M.: Simulating snow maps for Norway: description and statistical evaluation of  
37 the seNorge snow model, *The Cryosphere*, 6, 1323-1337, 2012.
- 38 Sato, A., Takahashi, S., Naruse, R., and Wakahama, G.: Ablation and Heat Balance of the  
39 Yukikabe Snow Patch in the Daisetsu Mountains, Hokkaido, Japan, *Annals of Glaciology*, 5,  
40 122-126, 1984.
- 41 Sigl, M., Jenk, T. M., Kellerhals, T., Szidat, S., Gaggeler, H. W., Wacher, L., Synal, H.-A.,  
42 Boutron, C., Barbante, C., Gabrieli, J., and Schwikowski, M.: Towards radiocarbon dating of  
43 ice cores, *Journal of Glaciology*, 55, 985-996, 2009.



- 1 Sollid, J. L., Holmlund, P., Isaksen, K., and Harris, C.: Deep permafrost boreholes in western  
2 Svalbard, northern Sweden and southern Norway, *Norwegian Journal of Geography* 54, 186–  
3 191, 2000.
- 4 Spindler, K.: *The Man in the Ice: The Preserved Body of a Neolithic Man Reveals the Secrets*  
5 *of the Stone Age*, Sutton, Stroud, 1994.
- 6 Suter, P. J., Hafner, A., and Glauser, K.: Lenk – Schnidejoch. Funde aus dem Eis – ein vor-  
7 und frühgeschichtliche Passübergang. , *Archäologie im Kanton Bern*, 6B, 499-516, 2005.
- 8 Sørđal, I.: Kartlegging av temperaturlilhøva i Gråsubreen og Juvfonne. , Master, Department  
9 of Geosciences, University of Oslo, Oslo, 81 pp.+ app. pp., 2013.
- 10 Tachon, M.: Thermal regimes and horizontal surface velocities on Hellstugubreen and  
11 Storbreen, Jotunheimen, Southern Norway, Master, Department of Geosciences, University of  
12 Oslo, Oslo, 99 pp. + app. pp., 2015.
- 13 UNESCO: Perennial ice and snow masses – a guide for compilation and assemblage of data  
14 for the World Glacier Inventory, *Technical Papers in Hydrology*, 1, 1970.
- 15 Vedeler, M., and Jørgensen, L. B.: Out of the Norwegian glaciers: Lendbreen—a tunic from  
16 the early first millennium AD, *Antiquity*, 87, 788-801, 2013.
- 17 Westermann, S., Schuler, T. V., Gislås, K., and Etzelmüller, B.: Transient thermal modeling  
18 of permafrost conditions in Southern Norway, *The Cryosphere*, 7, 719-739, 2013.
- 19 Winsvold, S. H., Andreassen, L. M., and Kienholz, C.: Glacier area and length changes in  
20 Norway from repeat inventories, *The Cryosphere*, 8, 1885-1903, 2014.
- 21 Zapf, A., Nesje, A., Szidat, S., Wacker, L., and Schwikowski, M.: <sup>14</sup>C measurements of ice  
22 samples from the Juvfonne ice tunnel, Jotunheimen, Southern Norway—validation of a <sup>14</sup>C  
23 dating technique for glacier ice, *Radiocarbon* 55, 571-578, 2013.
- 24 Zhang, Y. L., Perron, N., Ciobanu, V. G., Zotter, P., Minguillón, M. C., Wacker, L., Prévôt,  
25 A. S. H., Baltensperger, U., and Szidat, S.: On the isolation of OC and EC and the optimal  
26 strategy of radiocarbon-based source apportionment of carbonaceous aerosols, *Atmos. Chem.*  
27 *Phys.*, 12, 10841-10856, 10.5194/acp-12-10841-2012, 2012.
- 28 Ødegård, R.: Ground and glacier thermal regimes related to periglacial and glacial processes:  
29 Case studies from Svalbard and southern Norway, 2, Dr. scient. thesis (in English),  
30 Department of Geography, Rapportserie i naturgeografi, University of Oslo, Norway., Oslo,  
31 44 pp. pp., 1993.
- 32 Ødegård, R., Nesje, A., Isaken, K., and Eiken, T.: Perennial ice patch studies – preliminary  
33 results from a case study in Jotunheimen, southern Norway, *Geophysical Research Abstracts*  
34 Vol. 13, EGU2011-12027, EGU General Assembly 2011, Vienna, 2011, 1,  
35  
36



1 Table 1.

2 Areal extents of Juvfonne derived from topographic maps, Landsat imagery, GNSS  
3 measurements by foot and digitising from orthohotos. \*Seasonal snow remaining along the  
4 extent.

5

Year	Date	Source	Area (km <sup>2</sup> )
1981		map	0.171
1984	10.08.1984	Orthophoto	0.208
1997	15.08.1997	Landsat	0.208
2003	09.08.2013	Landsat	0.150
2004	12.08.2004	map	0.187
2010	25.08.2010	GNSS	0.149
2011	02.08.2011	GNSS	0.150
2011	17.09.2011	Orthophoto	0.127
2012	12.09.2012	GNSS	0.160
2013	12.08.2013	GNSS	0.151
2014	09.09.2014	GNSS	0.101
2015	11.09.2015	GNSS	0.186*

6

7



1 Table 2. AMS radiocarbon dates from the ice tunnels and ice samples from ice patch surface.

2  
3  
4  
5  
6  
7  
8  
9  
10  
11  
12  
13  
14  
15  
16  
17  
18  
19  
20  
21  
22  
23  
24  
25  
26  
27  
28  
29  
30  
31  
32  
33  
34  
35  
36  
37  
38  
39  
40  
41  
42  
43  
44  
45  
46  
47  
48  
49  
50  
51  
52  
53  
54  
55  
56  
57  
58  
59  
60  
61  
62

**Ice tunnel 1 (opened 2010)**

Lab. no.	Dated material	Radiocarbon age BP	Median probability	Calibrated ages	
				1 sigma (68.3%)	2 sigma (95.4%)
Poz-37877	Organic remains	1095 ± 30	CE 949	CE 945-987	CE 890-1012
Poz-37879	Organic remains	1420 ± 30	CE 627	CE 612-651	CE 582-660
Poz-39788	Reindeer dung	1480 ± 30	CE 586	CE 557-614	CE 539-644
Poz-37878	Organic remains	1535 ± 30	CE 511	CE 532-569	CE 428-592
Poz-36460	Organic remains	2960 ± 30	BCE 1172	BCE 1218-1125	BCE 1262-1072

Radiocarbon dates on carbonaceous aerosols trapped in the 'clean' ice matrix (Paul Scherrer Institute, Villigen, Switzerland; Zapf et al., 2013: Radiocarbon 55 (2-3), 571-578)

Lab. no.	Radiocarbon age BP	Median probability	Calibrated ages BP (=AD 1950)		Comments
			1 sigma (68.3%)	2 sigma (95.4%)	
JUV3_1 42845.1	-940 ± 95 BP	-42 BP (1950)	-42 - -47 BP		Sample from ice patch surface
JUV3_2 42845.2	-723 ± 113 BP	-48 BP	-46 - -53 BP		Sample from ice patch surface
JUV3_3 42845.3	-1157 ± 102 BP	-36 BP	-8 - -42 BP		Sample from ice patch surface
JUV3_4 42845.4	-1221 ± 116 BP	-34 BP	-8 - -41 BP		Sample from ice patch surface
JUV-3 2010 mean	-1010 ± 107 BP	-41 BP	-40 - -45 BP (Modern)		Samples from ice patch surface

Lab. no.	Radiocarbon age BP	Median probability	Calibrated ages	
			1 sigma (68.3%)	2 sigma (95.4%)
JUV2_1 43443.1	1021 ± 205	CE 995	CE 861-1211	CE 640-1312
JUV2_2 43443.2	1874 ± 665	CE 45	BCE 592-CE 724	BCE 1433-CE 1329
JUV2_3 43443.3	1121 ± 321	CE 891	CE 640-1221	CE 251-1432
JUV2_4 43443.4	1126 ± 284	CE 892	CE 652-1169	CE 381-1405
JUV2 2010 Mean	1286 ± 409	CE 720	CE 378-1165	BCE 169-1442
JUV1_1/2 43442.1	3875 ± 342	BCE 2353	BCE 2776-1924	BCE 3138-1501
JUV1_3 43442.2	2144 ± 303	BCE 200	BCE 541-CE 172	BCE 846-CE 475
JUV1_4 43442.3	2647 ± 711	BCE 834	BCE 1641-CE 69	BCE 2588-CE 775
JUV1 2010 Mean	2889 ± 488	BCE 1105	BCE 1643-471	BCE 2346-CE 85

**Ice tunnel 2 (opened 2012)**

Lab. no.	Dated material	Radiocarbon age BP	Median probability	Calibrated ages	
				1 sigma (68.3%)	2 sigma (95.4%)
Poz-56952	Organic remains	2025 ± 30	BCE 25	BCE 53-BCE 21	BCE 111-CE 55
Poz-56953	Organic remains	3490 ± 35	BCE 1816	BCE 1831-1767	BCE 1904-1737
Poz-56954	Organic remains	4595 ± 35	BCE 3367	BCE 3376-3340	BCE 3382-3326
Tra-4427	Organic remains	5044 ± 100	BCE 3841	BCE 3954-3761	BCE 4001-3645
Poz-56955	Organic remains	5800 ± 40	BCE 4651	BCE 4711-4606	BCE 4729-4544

Radiocarbon dates on carbonaceous aerosols trapped in the 'clean' ice matrix sampled and dated in 2015 (Paul Scherrer Institute, Villigen, Switzerland)

Lab. no.	Radiocarbon age BP	Median probability	Calibrated ages	
			1 sigma (68.3%)	2 sigma (95.4%)
juv1-1 4184.1.1	5909 ± 248	BCE 4807	BCE 5061-4495	BCE 5373-4319
juv1-2 4380.1.1	6300 ± 138	BCE 5255	BCE 5384-5203	BCE 5525-4932
juv2-1 4185.1.1	6521 ± 217	BCE 5455	BCE 5664-5292	BCE 5877-4985
juv2-2 4381.1.1	6565 ± 135	BCE 5514	BCE 5628-5463	BCE 5730-5293
juv3-1 4186.1.1	7306 ± 232	BCE 6178	BCE 6418-5988	BCE 6602-5725
juv3-2 4382.1.1	6682 ± 227	BCE 5609	BCE 5812-5463	BCE 6049-5207
juv5-1 4187.1.1	7293 ± 219	BCE 6166	BCE 6397-5987	BCE 6532-5734
juv5-2 4383.1.1	6405 ± 230	BCE 5336	BCE 5564-5204	BCE 5735-4800
juv 0 (2015) Mean	6623 ± 210	BCE 5555	BCE 5733-5359	BCE 5983-5206



1 Table 3.

Sample blocks	Sample description
1	JUV 0_1 and JUV 0_2: the side of the ice step with plant fragment layer. Clear ice divided into two sub samples. Since there was no place to cut off further ice, the other samples were taken from the wall on the left side of the corner where the ice step is located.
2	JUV 0_3 and JUV 0_4: divided into two subsamples. This sample broke into pieces during cutting, but it is clear ice.
3	JUV 0_5 and JUV 0_6: nice and clear ice block cut at the right of sample 4. It was divided into two subsamples.
4	This ice block contains a lot of dark organic material. For the moment it is stored in the cold room and has not been processed. It could be measured with the conventional radiocarbon procedure and it is possible to separate some clear ice for the carbonaceous dating approach.
5	JUV 0_7 and JUV 0_8: clear ice cut inside the hole left after cutting sample 3. It was divided into two subsamples.

2

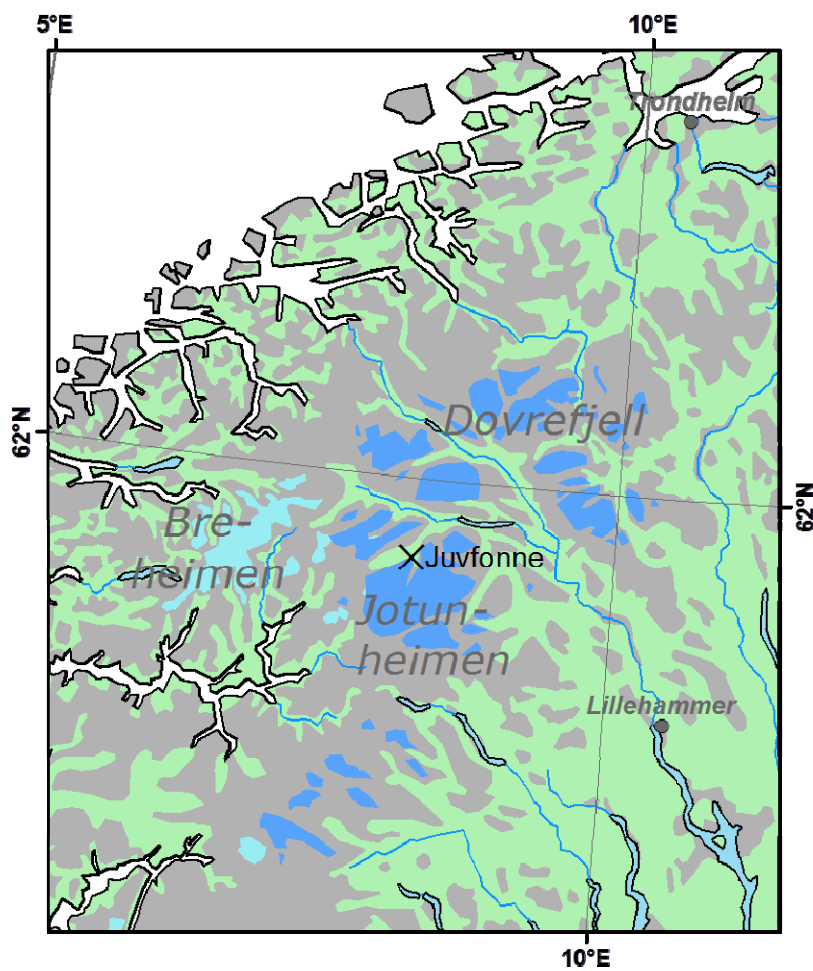
3



- 1 Table 4
- 2 Key statistics for the first order polynomial fit of snow accumulation (deviation from mean
- 3 each year) in the period 2010-2015.

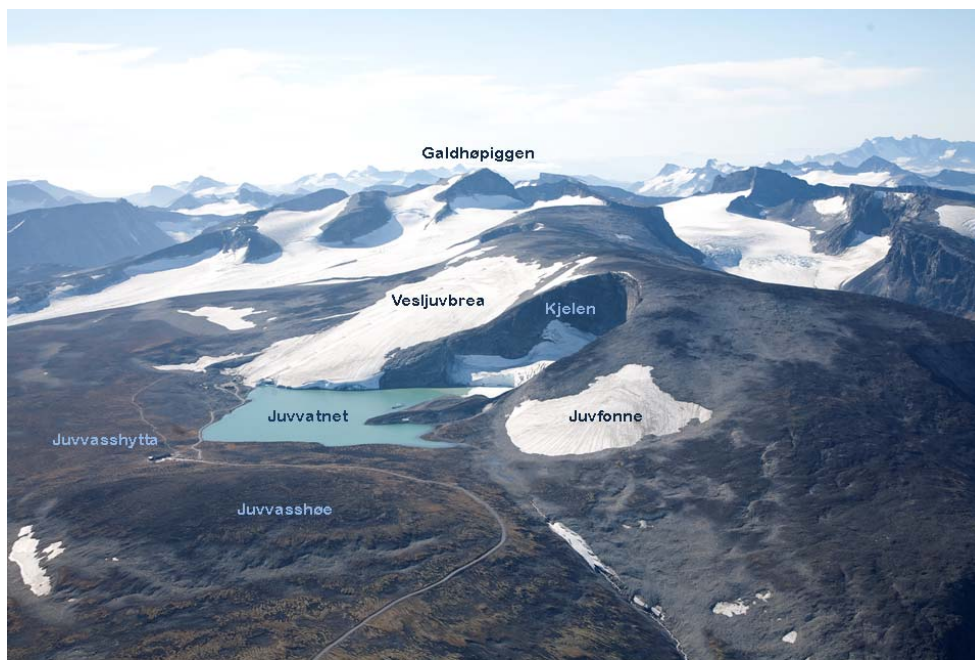
Sources of variation	Sums of squares	Degrees of freedom	Mean Square	F-test
First order polynomial regression	0.656	2	0.328	6.339
Deviation	11.847	232-2-1 (229)	0.052	
Total variation	12.503	232-1 (231)	0.054	

- 4
- 5

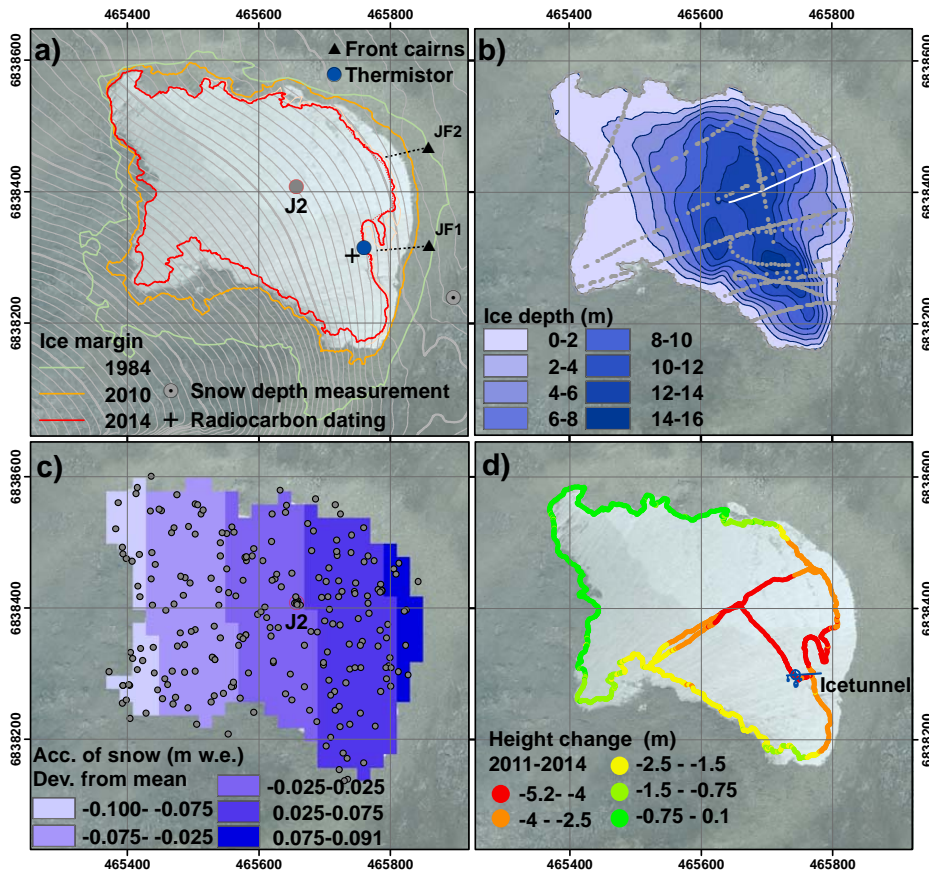


1  
2  
3  
4  
5  
6

Figure 1. The field site Juvfonne (marked with X) in central southern Norway. Dark blue is permafrost areas, light blue is glaciers. Permafrost extent generalized from Lilleøren et al. (2012).

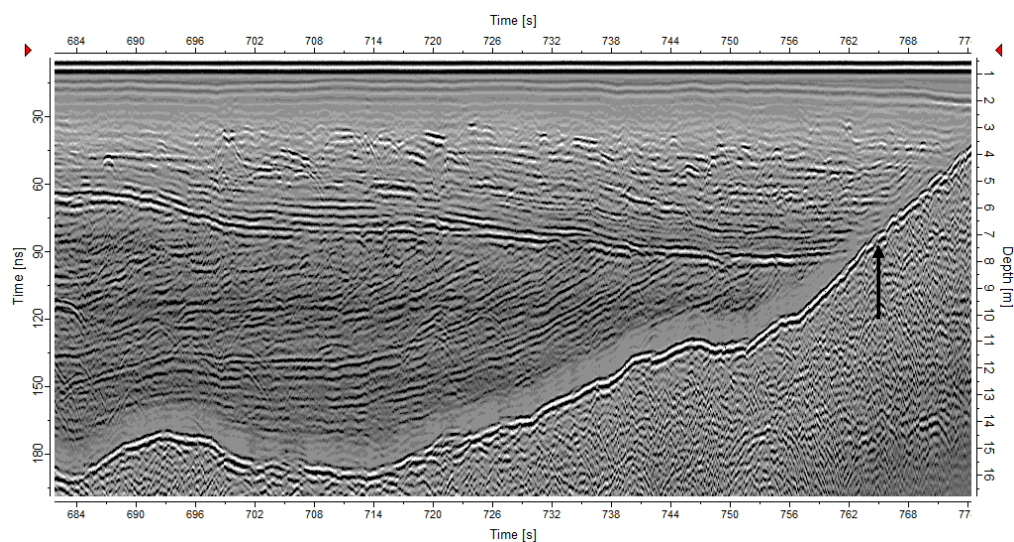


1  
2 Figure 2. Overview picture of Juvfonne and the Juvflye area including Kjelen. Juvvatnet,  
3 Juvvasshytta, Vesljuvbreen and the P30 and 31 Permafrost and Climate in Europe (PACE)  
4 boreholes at Juvvasshøe. Also visible is the highest mountain of Norway, Galdhøpiggen  
5 (2469 m a.s.l.). Photo: Helge J. Standal.  
6



1

2 Figure 3. Maps of Juvfonne with ortofoto from September 2011 as background, a) ice  
 3 margins, position of front measurements (JF1 and JF2- see figure 14), position of mass  
 4 balance stake J2, position of thermistor for ice temperature measurements (Fig. 12) and  
 5 position of the oldest radiocarbon dating and position of snow depth measurement station, b)  
 6 interpolated contours of bed topography relative to ice thickness in September 2011 (grey  
 7 markers are radarpoints used in the interpolation) and position of the georadar track in Fig. 4 -  
 8 white line, c) grey markers are snow depth measurements (2010-2015), the raster map shows  
 9 a first order polynomial fit to the deviation from mean accumulation each year (see table 3 for  
 10 details) d) height differences along GNSS tracks in 2014 relative to ice surface from laserdata  
 11 in 2011 and positions of ice tunnel excavated in 2012.



1  
2  
3  
4  
5  
6

Figure 4. Example of 500 MHz Georadar profile. The position of the track shown in figure 3b. The arrow shows minimum front position in September 2014 (Ice velocity: 168 m  $\mu$ s<sup>-1</sup>, adjustment velocity: 300 m  $\mu$ s<sup>-1</sup>, automatic gain control, scale factor 5000).



1  
2  
3  
4  
5  
6  
7

Figure 5. Photo of angular discontinuity at the wall of the 2010 ice tunnel, as also observed on the georadar data (Fig. 4). The upper layering is parallel to the surface of Juvfonne. Radiocarbon dating of the upper part showed modern age. Width of picture is approximately 0.4 m.

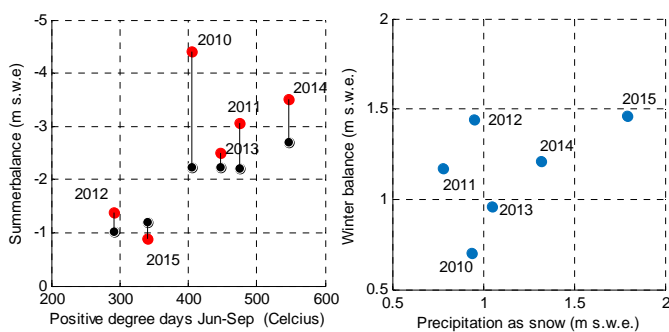


1  
2  
3  
4  
5  
6  
7  
8  
9

Figure 6. Photos of Juvfonne 17 September 2014 (upper) and 10 September 2014 (lower) showing the pre ‘Little Ice Age’ surface exposed in central and southern parts of the ice patch (left side). The area on Juvfonne in the north-west (right side) is interpreted to be ice of modern age. The entrance of the ice tunnel is sitting on a small ridge that might be ice cored (left side lower image). The collapsed 2010 tunnel is to the left of the entrance. Photo: Glacier Archaeology Program/Oppland County Council (upper) and L. M. Andreassen (lower).



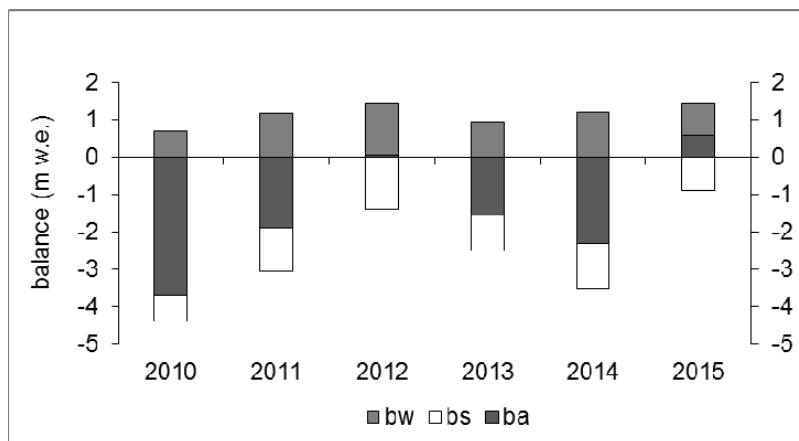
1



2

3 Figure 7. Summer (left) and winter (right) balance plotted against summer temperature  
4 (positive degree days) and precipitation as snow, respectively. For the summer balance the  
5 black markers are calculated melt using a degree-day model with typical values calibrated  
6 from nearby glaciers (3.5 mm/°Cday for snow and 7.5 mm/°Cday for ice). Winter  
7 precipitation is obtained from seNorge (Engeset et al., 2004).

8



1  
2  
3  
4  
5

Figure 8. Mass balance measurements at stake J2 on Juvfonne: bw – balance winter, bs – balance summer, ba – annual (net) balance. See figure 3a for position of stake.



1

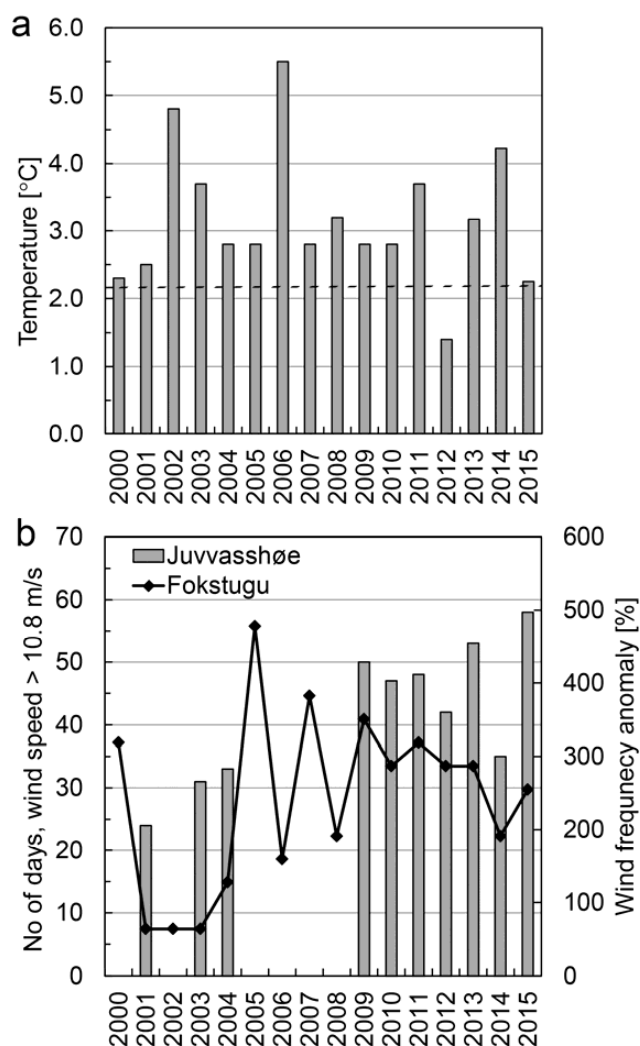
2

3 Figure 9. Front position of Juvfonne measured at two locations relative to the 2010-front.

4 Minima are observed in 2011 and 2014. The front retreat 2009-2014 was measured to 69 m.

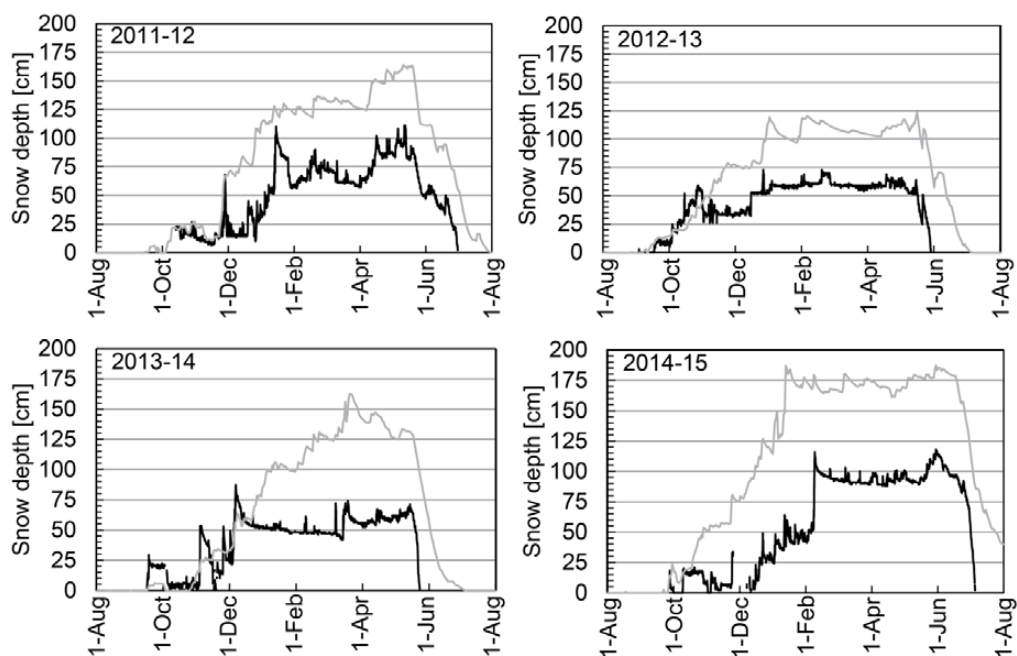
5 For position of measurements, see figure 3a. Red - JF1, Green – JF2.

6



1  
 2  
 3  
 4  
 5  
 6  
 7  
 8  
 9

Figure 10. Meteorological data from the station at Juvvasshøe (750 m from the front of Juvfonne) and Fokstugu 70 km NE a) Juvvasshøe June-September mean Air Temperature. The black dotted line denotes the 1971-2000 mean, obtained from the interpolated seNorge dataset (Engeset et al. 2004). b) Number of days for the period June-September with strong breeze or higher (wind speed above 10.8 ms<sup>-1</sup>) at Juvvasshøe (grey bars) and at Fokstugu (black line), the latter shown as anomaly (in %, right axes) with respect to 1971-2000 mean.

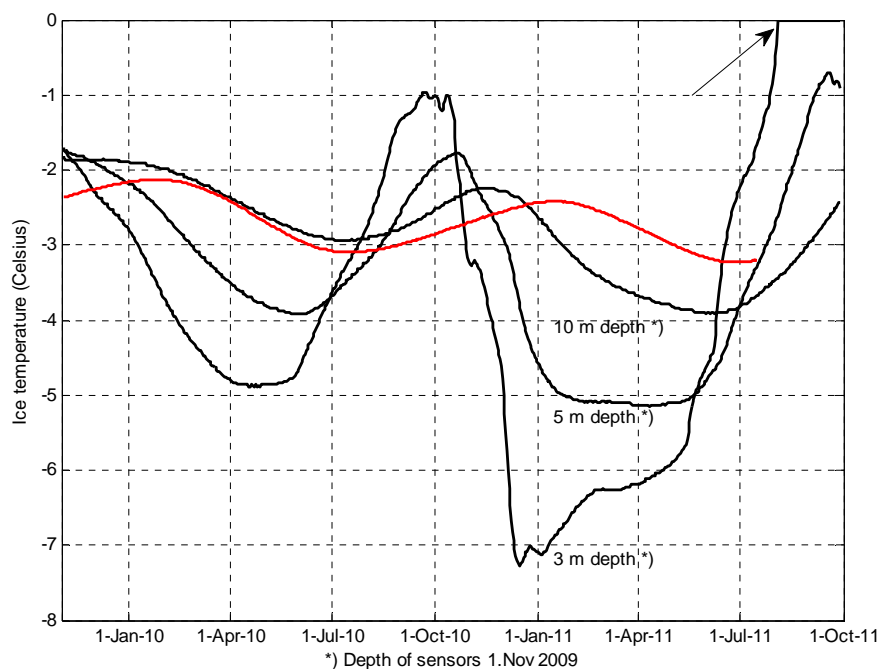


1

2

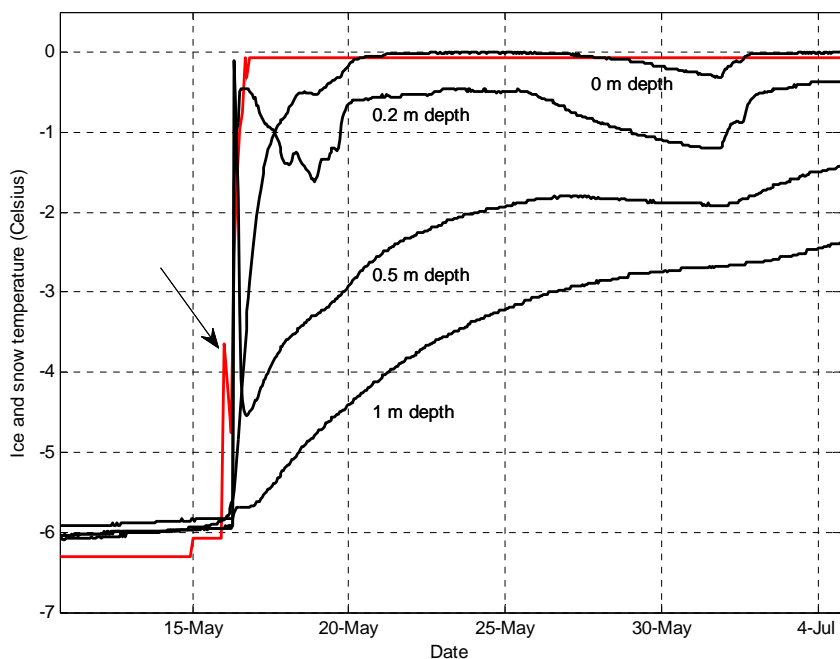
3 Figure 11. Hourly snow depth measurements (black lines) from the station 95 m from the  
4 front of Juvfonne (see Figure 3a for position). Grey lines show modelled daily snow depth  
5 from seNorge (Engeset et al. 2004).

6



1  
2  
3  
4  
5  
6  
7  
8

Figure 12. Temperature for November 2009-September 2011 in a 10 m deep borehole in the Juvfonne ice patch (see Figure 3a for position). The red line is the temperature at 10 m depth in the P31 permafrost borehole 750 m north from the ice patch (see Figure 2 for location). Arrow points to the time when the sensor placed at 3 m depth in autumn 2009 melted out. The entire thermistor string melted out in mid-September 2014.



1

2

3 Figure 13. Plot of temperature measurements in ice and snow at the onset of thaw in May  
4 2010 (position at the thermistor shown in figure 3a). The depth reference is the ice surface the  
5 previous autumn. The red line is the snow temperature 0.25 m from the base of the snow  
6 cover. The arrow point the first signal of surface meltwater refreezing close to the base of the  
7 snow cover.

8



1

2

3 Figure 14. Photo from the old ice tunnel excavated in 2010 showing the layering in the ice  
4 and position of two samples for radiocarbon dating. Photo: Klimapark2469 AS.

5